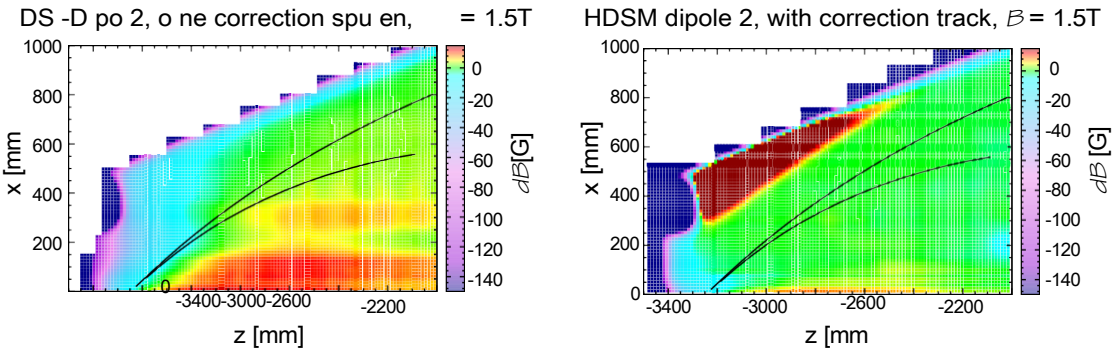

Figure 2.14:
Section of the field map of HDSM dipole 2 at 1.5 T (left without, right with correction coil, [46]).

related) of about 2.4° to 4.8°.

2.6 High-frequency monitors

High-frequency monitors (HFMO) of various types are widely used in accelerator facilities and can cover a range of applications. With x/y monitors (XYMO), the position relative to the geometric centre of the resonator can be determined, p/i monitors (PIMO) provide information about the phase and intensity of the beam. For MAMI, an RF monitor system was already planned from the beginning of the planning in order to be able to centre the recirculated beams as they cross the linac [11]. The monitor system described there still forms the basis of beam diagnostics with RF resonators at MAMI. Therefore, the basics are briefly summarised here.

2.6.1 Basics

The resonators represent a shunt impedance r_S for the beam. Accordingly, the resonator extracts a high-frequency power of $P = i^2 \cdot r_S$ from the beam. An antenna with a coupling constant κ decouples part of the power from the resonator and thus loads it accordingly. In beam steering systems where the beam crosses the monitor only once at a time, high quality monitors ($Q_0 = \nu/\Delta\nu$ 10000) are installed and detect the beam position, phase or intensity with up to a few kHz bandwidth.

2.6.2 Various functions of the HF monitors

In a cylindrical resonator, the resonance frequencies of the different TM modes are generally determined by the radius R and the length L (X_{mn} is the *nth* zero of the mth Bessel function):

$$f_{mnp} = \frac{c}{2\pi\sqrt{\mu_r \epsilon_r}} \sqrt{\left(\frac{X_{mn}}{R}\right)^2 + \left(\frac{p\pi}{L}\right)^2} \qquad (2.2)$$

If the resonance frequency f_{mnp} matches the bunch frequency or an integer multiple of it, the TM_{mnp} mode can be excited. Two types of monitor are used in the HDSM, in which either the TM_{010} mode (phase monitor) or the TM_{110} mode (position monitor) can be excited. Figure 2.15 schematically shows a resonator with the electric fields of a TM_{010} and a TM_{110} mode.

Phase and intensity monitor (PIMO)

For a phase or intensity monitor, the TM_{010} mode is used, whose am- plitude is excited practically independently of the beam position. For a PIMO, the output RF power P_{HF} depends on the beam intensity i, the constant shunt *impedance* $r_{S\,010} = r_{m\,010}$ and the *coupling* constant κ:

$$P_{HF}(p/i) = (i^2 \cdot r_{S010}) \cdot \frac{\kappa}{(\kappa+1)^2} = i^2 \cdot r_{m\,010} \cdot \frac{\kappa}{(\kappa+1)^2} \qquad (2.3)$$

Position monitor (XYMO)

The next mode TM_{110} is excited in proportion to the beam deposition and is thus ideally suited for measuring depositions from the target position, which is at the centre of an x/y position monitor [48, 49]. For an XYMO, however, the shunt impedance is a function of the deviation x from the centre of the resonator and a *scaling* constant k in [*mV/mm/µA*]:

$$r_{S\,110} = r_{m\,110} - k\,x^{22} \qquad (2.4)$$

Thus the decoupled power is:

$$P_{HF}(x/y) = (i^2 \cdot r_{S110}) \cdot \frac{\kappa}{(\kappa+1)^2} = i^2 \cdot r_{m\,110} \cdot \frac{\kappa}{(\kappa+1)^2} \cdot k\,x^{22} \qquad (2.5)$$

Information only about the centre of gravity of the load

Bunch-to-bunch or even intrabunch diagnosis is impossible with such resonators, because the loaded quality of the monitors is usually Q_L 10 and thus the individual bunches cannot be resolved by the monitor. The further signal processing (especially the down-conversion) also prevents in principle that higher Fourier components are detectable, which result from a differently extended charge distribution. Therefore, only statements about the charge centre of gravity can be made.

2.6.3 Analogue signal processing

The resonant frequency of the desired TM mode of all resonators is at the MAMI frequency of 2.449532 GHz or an integer multiple of it. Therefore, they first provide an RF signal that corresponds to the resonant frequency of the monitor, but whose phase is rigidly coupled to MAMI's master oscillator by the beam bunches. With typical beam currents between 1 nA and 100 μA, the output power ranges from a few pW to a few mW. Therefore, the processing (demodulation, Figure 2.15) of the RF signals is always done in close proximity to the installed monitors.

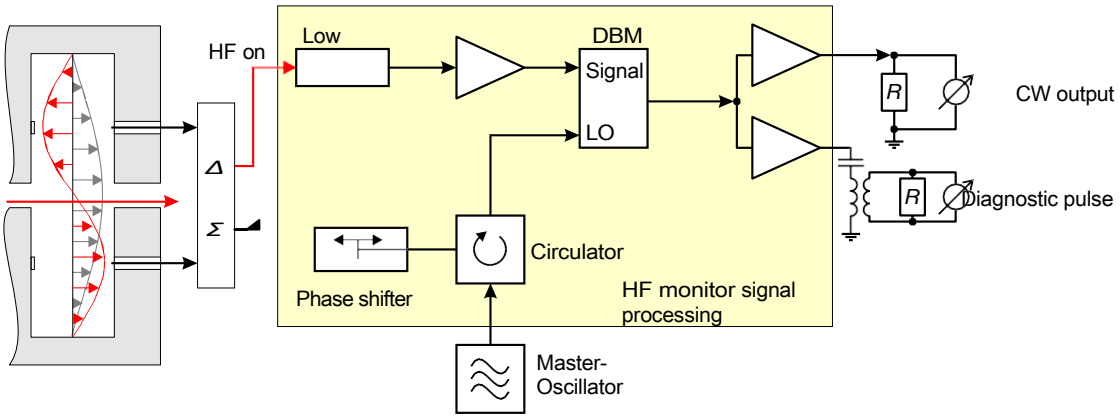

Figure 2.15:
Signal processing of the RF monitor signals [48]: The electron beam in the resonator shown (left) is indicated by the red dashed arrow. Two RF modes are also shown there (TM$_{\square\square\square}$ grey for PIMOs and TM$_{\square\square\square}$ red for XYMOs). With the XYMO, two antennas and a hybrid are used before the RF signal is fed to further processing. With the PIMO, there is only one antenna and no hybrid at this point. The master oscillator supplies the mixer ("double balanced mixer", DBM [50]) with the RF reference via a phase shifter in order to demodulate the RF signal of the monitor.

The signals are first filtered through a low-pass filter in order to remove all interfering higher

frequency components before the subsequently amplified signal is mixed in a double-balanced mixer ("DBM") with the reference phase of a "local oscillator" (LO) is mixed. The LO is derived directly from the master oscillator via a phase shifter (see figure 2.15). Because both frequencies are identical, depending on the setting of the reference phase, this circuit corresponds to a phase- or amplitude detector and the DC output voltage is proportional to $\sqrt{P_{HF}}$. Mixing down to the baseband (homodyne or "zero IF") allows a much simpler set-up of the signal processing compared to autodyne measurement (section 2.4.3), as the circuits for the intermediate frequency can be dispensed with here. The output voltage is then available as an analogue signal U_{HFMO} for various applications and can, for example, be displayed on an oscilloscope or digitised with fast ADCs. In contrast to autodyne phase measurement, this concept achieves much larger bandwidths on the DC output side, which can reach 100 MHz if the circuit is designed accordingly.

The behaviour of 2.45 GHz electronics with regard to phase and amplitude variations has been investigated and shows that the deviations from the ideal behaviour according to equation 2.6 are significantly smaller than 2% [48]:

$$U_{HFMO} \sim \sqrt{P_{HF}} \cdot \cos(\varphi - \varphi)_{LO} \qquad (2.6)$$

Thus, if according to equation 2.6 the phase difference of the phase φ *of* the electron beam to the reference phase φ_{LO} is minimised (or $\cos(\varphi - \varphi_{LO}) = \pm 1$) and then the measured signal voltage is normalised to the beam intensity i, the output voltages of the monitors can be converted into physical quantities (e.g. $k = 1$ *mV/mm/µA*):

$$x = k \cdot \frac{U_{HFMO}}{i} = k \cdot \frac{\sqrt{P_{HF}}}{i} \qquad (2.7)$$

The PIMO is used in a slightly different way. Depending on the phase difference, it serves either as a phase monitor ($\cos(\varphi - \varphi_{LO}) = 0$, with constant beam current) *or as an* intensity monitor ($\cos(\varphi - \varphi_{LO}) = \pm 1$, with constant beam phase). If the monitor signal is distributed to two of the analogue signal processing systems (Figure 2.15) in parallel, whose reference phases differ by $90°$, both phase and intensity can be recorded simultaneously.

2.6.4 HF monitors in the recirculating accelerator

Each linac of RTM1, RTM2, RTM3 and HDSM is equipped with one XYMO each before and after the acceleration sections (input and output) (Figure 1.7 shows the installation in the HDSM), which can be used to bring the beam onto the target path. A PIMO provides the necessary phase and intensity information.

In order to use the HF monitors on the lens axes of the microtrons, they must be able to clearly separate the individual circuits. This only works with a

pulsed beam, but this is not used in experimental operation. This diagnostic pulse of length τ_{dp} , several tens of bunches long, must be shorter than the shortest round-trip time τ_{RTM} of the microtrons so that the recirculated beams of different energies do not overlap in a monitor. This is most critical in RTM1, where the time of flight for the first circulations is only about 15 ns. This defines both the characteristics of the diagnostic pulse and the minimum bandwidth requirement of the monitor system: The diagnostic pulse must be about 10 ns long (separation of the circulations in RTM1) and the beam current must be about 100 µA (sensitivity); a signal bandwidth of 200 MHz must be guaranteed for the entire system from the RF monitor to the digitisation with fast ADCs. The "low-Q" resonators used with a loaded Q <100 are capable of generating these fast signals.

This makes the RF monitors of the microtrons in pulse mode ideally suited for providing phase, intensity and deposition information of the individual circulations with comparatively little technical effort when installed on the linac axis.

The average beam current in diagnostic pulse mode is 1 nA/kHz, so that beam losses during measurements do not cause any major damage. Most of the investigations were carried out in diagnostic pulse mode at frequencies between 1 kHz and 10 kHz.

Evaluation of the monitor signal

The diagnostic pulse is generated as a kind of square wave function of length τ_{dp} , so the course of the signal voltage $u(t)$ should ideally also be square wave. Here, however, the finite quality of the resonator and much more the bandwidth of the signal processing as a low-pass filter come into play. Therefore, the measured signal curve corresponds more to the curve in Figure 2.16; however, since not only a low-pass filter is used in the signal processing, the curve is smoothed even more, so that the range of the maximum can be approximated well by a parabola, in order to be able to determine, for example, an exact time *reference* T_i for each cycle [51].

Assuming that the complete signal processing chain is represented as a PT_1 link or a linear time-invariant (LZI) system that is subject to the superposition principle [52], a quantity proportional to the power originally deposited in the resonator can be determined by measuring the measured pulse around its maximum T_i in a interval $[T_i - \frac{1}{2}\tau_{dp}, T_i + \frac{1}{2}\tau_{dp}]$ is summed up or integrated.

$$x_i \sim \int_{t=-\frac{1}{2}\tau_{dp}}^{\frac{1}{2}\tau_{dp}} u(T_i + t)\, dt \qquad (2.8)$$

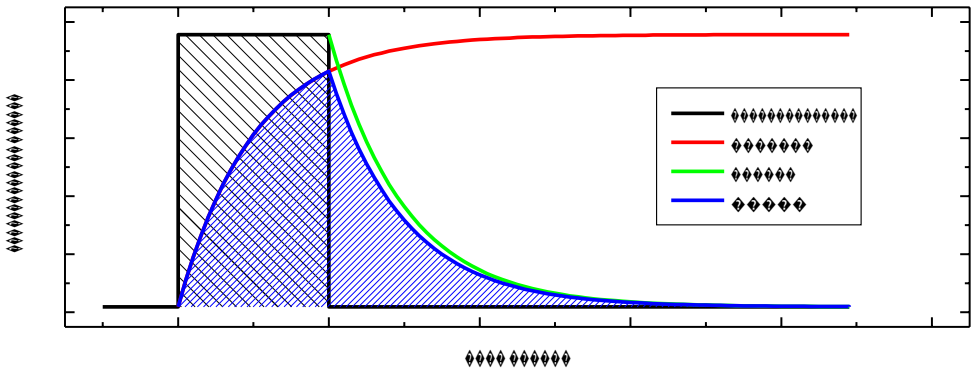

Figure 2.16: System response of an LZI system (here: low pass) to a square wave pulse

2.6.5 Data collection

In all MAMI microtrons, a corresponding system consisting of two x/y monitors and one p/i monitor has been used for a long time to centre the recirculated beams on the linac axis and to control and eliminate the synchrotron oscillations.

Therefore, from RTM1 to RTM3 alone, six monitor signals are available each. However, because the monitors are passed through sequentially in time by the beam, the signals of similar monitors of the different microtrons (e.g. the horizontal position at each entry into the linac) can be combined into one signal when switching between the monitors (i.e. from RTM1 to RTM2 to RTM3 to HDSM) in time synchronisation with the electron beam (i.e. after the beam leaves one microtron and before it enters the next). The rigidly connected multiplexer used so far was no longer able to integrate the many additional signals of the HDSM. Therefore, a new programmable multiplexer was developed by the Institute's electronics department. This now allows a much more flexible configurable distribution of the monitor signals to up to eight ADC channels (Figure 2.17). With this equipment, it is possible to acquire the relevant x/y and p/i signals of all microtrons simultaneously with only one diagnostic pulse.

Currently, a maximum of four ADC modules with two channels each from Acqiris (DC241A, [54]) are used. These optimally fulfil the requirements placed on data acquisition:

- 1 GHz analogue bandwidth
- 2-4 GS/s sampling rate
- A short dead time (<800 ns) allows sequential acquisition of up to 200 trigger events including time information in one "shot".

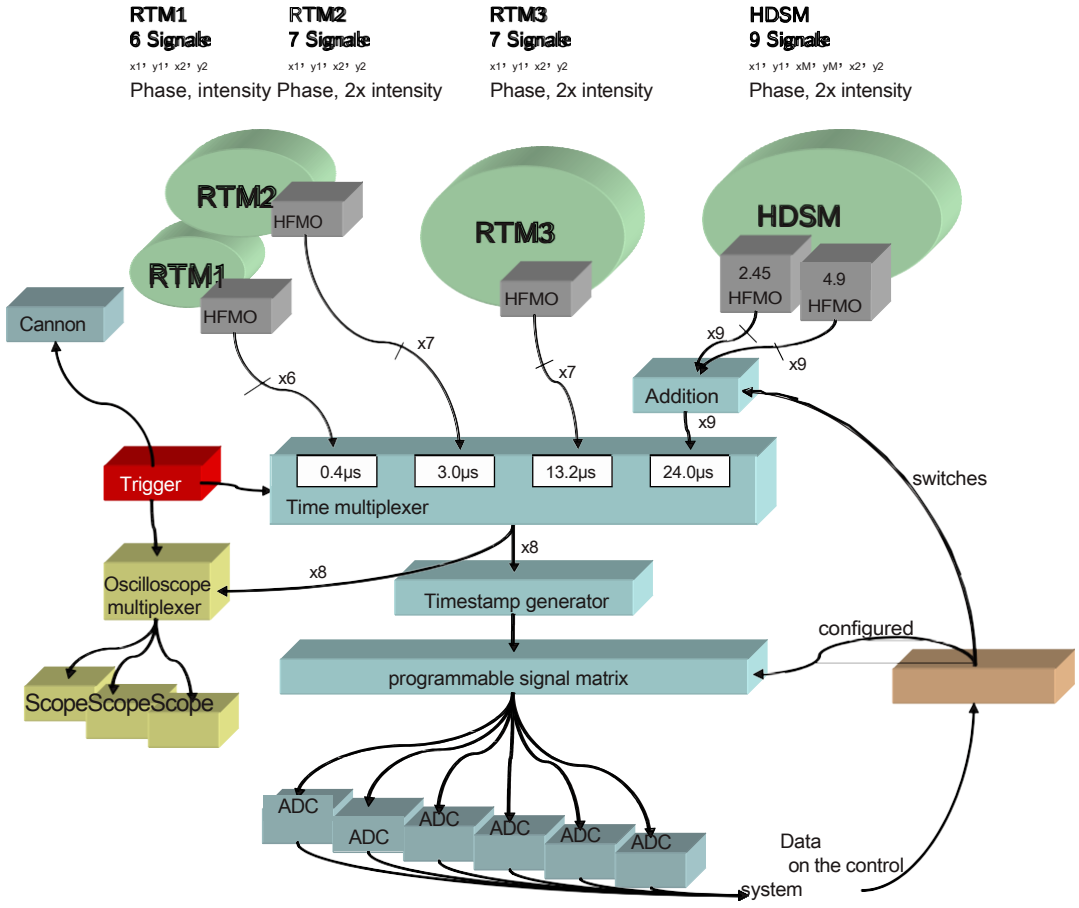

Figure 2.17:

Signal paths of the microtron RF monitors [53]: The diagnostic pulse leaves the gun and is accelerated by the individual microtrons. The RF monitors provide the corresponding signals and are brought to the RF monitor multiplexer. There, an additional time stamp is added to the signals. For distribution to the ADC channels, a programmable signal matrix is used to which all signals are permanently applied. The same applies to the oscilloscope multiplexer, which is used for the real-time analogue display of the monitor signals on the oscilloscopes in the operating room.
The ADC software in the control system automatically ensures the optimal configuration of the signal matrix and provides the processed measurement data.

- Trigger resolution of 5 ps through "trigger time interpolation" (TTI)
- 1 GHz auto-synchronisation bus (ASBus) to synchronise trigger and sampling clock to the different modules
- PCI bus for fast readout of the modules with up to 100 MB/s

The ADCs are operated with a sampling rate of 500 MS/s. Here again, the RTM1 is determinative, because at a lower sampling rate the individual cycles can only be poorly reproduced (Figure 2.18). The ADCs can be operated at a maximum sampling rate of 2 GS/s, but the advantage of the only minimally improved resolution in the RTM1 is quickly cancelled out by the four times greater amount of data per diagnostic pulse: Already in the RTM2, the individual pulses are at least 40 ns apart and thus far enough apart that a higher sampling rate brings no advantages.

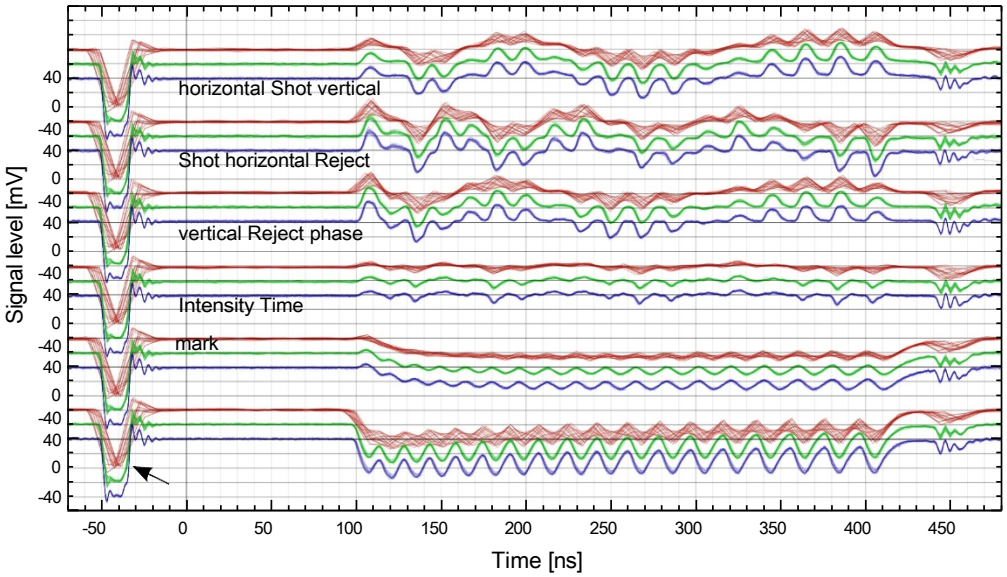

Figure 2.18:
Sampling rates in RTM1 from 0.1 GS/s to 2 GS/s: 0.1 GS/s (red, +40 mV offset), 0.4 GS/s (green, +20 mV offset), 2.0 GS/s (blue, 0 mV offset). Shown are (from top to bottom) the RF monitor signals of the RTM1: horizontal/vertical before the linac (shot), horizontal/vertical after the linac (reject), phase and intensity. In each case 20 diagnostic pulses in 20 ms were digitised. From a sampling frequency of 0.4 GS/s, the individual rotations can be well separated.

The flight time (and thus also the length of the signal train) from the shot RTM1 to the reject of the HDSM is about 24 μs. At 500 MS/s, this means a data volume of approx. 12000 bytes per signal per diagnostic pulse. However, 256 kByte of internal memory is available to each ADC channel, so that up to 20 consecutive diagnostic pulses can be digitised into the memory and processed in one operation. In practice

it has proved useful to distribute these 20 pulses evenly over a mains voltage period of 20 ms (50 Hz), as the influence of the mains hum is then efficiently suppressed (Figure 2.19). This results in a diagnostic pulse frequency of 1 kHz, which, however, would severely impair the synchronous display of the signals on an analogue oscilloscope in the control room (too low intensity)[6]. In order to be able to use the highest diagnostic pulse frequency of 10 kHz, the ADC trigger was extended by a programmable substitution, so that the desired number of trigger events are evenly distributed over 20 ms.

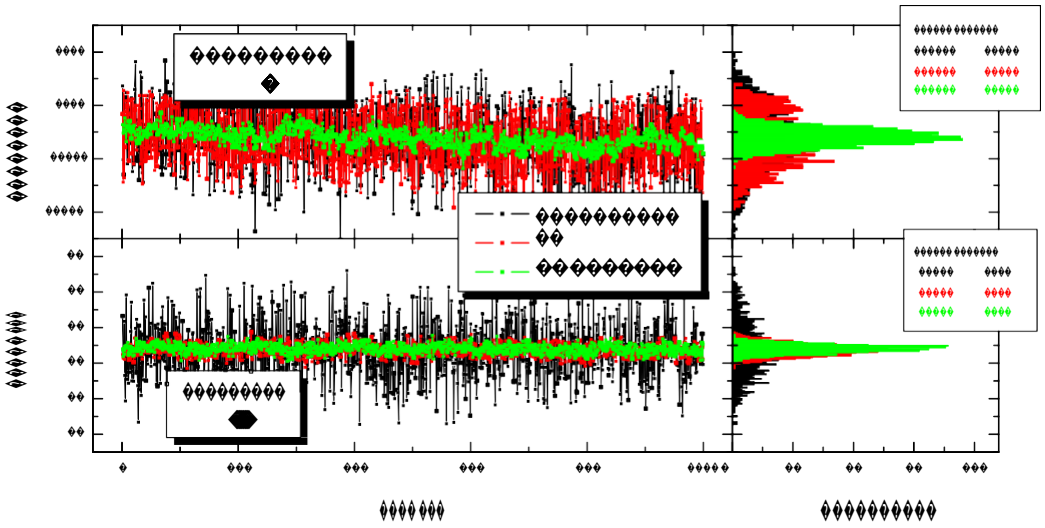

Figure 2.19:

Comparison of the scattering of 1000 HF monitor measurements each (HDSM shot; horizontal/phase): The influence of the mains hum is effectively suppressed by a factor of 5-10 by averaging over 20 ms in each case.
At the same time, the stability of the operating parameters is shown here, since, for example, the phase variation ◆◆ remains significantly smaller than *** (standard deviation, green) over a period of 15 minutes. This stability is assumed in the measurements (chapter 4).

The automatic interpolation of the real trigger time (TTI) is very helpful. With a sampling rate of only 500 MS/s, the individual ADC samples are already 2 ns apart. Since the internal reference clock of the ADCs does not match the

[6A] modern digital oscilloscope cannot be used for beam diagnostics of the microtrons because the relatively low screen resolution makes the simultaneous display of all 90 revolutions of the RTM3 look unsatisfactory. Therefore, an analogue oscilloscope is used in conjunction with the new oscilloscope multiplexer. With each new diagnostic pulse, this passes one of the normally six signals to the oscilloscope for 6-channel representation. Especially in the RTM1, this means that from each signal with a frequency of 1/6 kHz, an interval of 300 ns from 1 ms can only be displayed very darkly.

canon trigger is synchronised, a trigger event can thus vary by ±1 ns. If simple averaging is then performed sample by sample, this reduces the usable signal bandwidth, which is illustrated in Figure 2.20. However, because the ADC hardware provides the trigger time much more accurately (5 ps according to the data sheet) regardless of the current sampling rate, the individual diagnostic pulses can first be interpolated to the real trigger time before averaging the data [54].

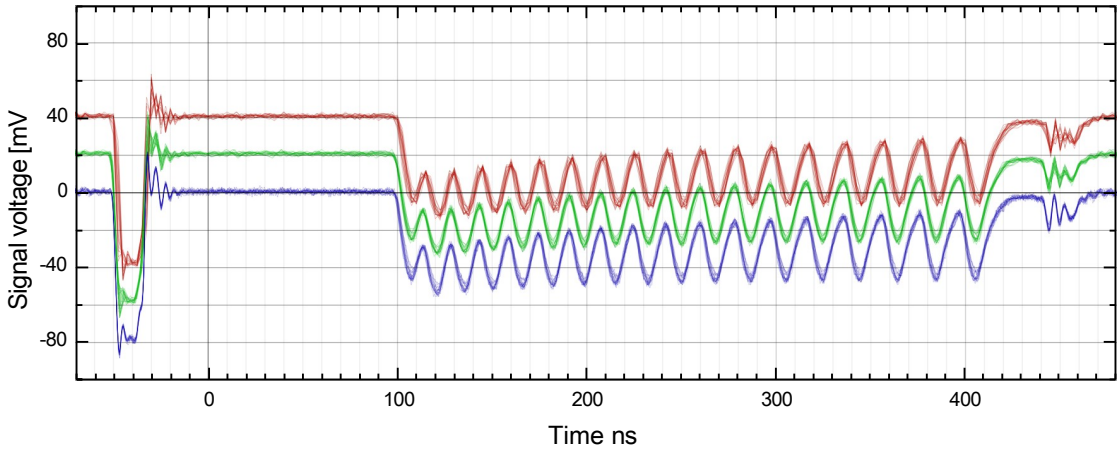

Figure 2.20:
TTI effect on intensity signal (RTM1) at 0.4 GS/s: 0.4 GS/s without TTI (red, +40 mV offset), 0.4 GS/s with TTI (green, +20 mV offset), 2.0 GS/s as comparison (blue). Especially the high-frequency parts in the signal course of the time marker (left) are clearly better reproduced by trigger interpolation, so that this functionality is used as standard. In each case 20 diagnostic pulses in 20 ms were digitised.

2.7 Data processing

The automated data processing of the RF monitor signals is an essential com- ponent in the operation of MAMI's microtrons. During normal operation, the system must function reliably to provide the required measurement data for optimisations of the correction magnets or the linac phases.

2.7.1 Interpretation and analysis of the signals

The signals from the RF monitors are always checked by the operator on the central oscilloscope during beam optimisation in routine operation. Because four position signals as well as the phase and intensity signals of all the microtrons are displayed in a six-channel display, it is practical that signal pulses of the same height are of similar size.

display beam deposits. Therefore, the individual levels of the monitors are approximately balanced by individual series resistors so that a deposit of 1 mm leads to a pulse height of about 50 mV.

However, the computer-aided data acquisition allows an individual calibration of the signals by determining the scaling constant k according to equation 2.7 for each x/y monitor individually by setting a well-defined beam deposition.

The intensity signal plays a special role in the data analysis by providing the time information T_i for the individual revolutions. Because in an optimised machine the remaining transverse deposit signals are too small, the individual circulations cannot be reliably separated with the x/y signals alone. Pulse processing is based on the long-proven strategy [53]:

- In order to obtain the exact time position T_i for revolution i, the local maxima in the signal curve $u(t)$ of the intensity signal that exceed a certain threshold are first determined.
- The signal is then adjusted by a parabola over the typical half-width of the pulse waveform of ±10 ns to obtain a position of the maximum that is less disturbed by noise.
- If the parameters of the parabola (height, distance of both zeros) make sense and the distance to the previous orbit T_{i-1} corresponds approximately to the orbital period, the orbital axis is found and the evaluation is continued.
- All signals are then integrated over the same interval at the corresponding temporal position according to equation 2.8; differences in running time (e.g. due to cable lengths) can easily be compensated for here. This determines the size of the pulse and thus also the physical measurand.

Furthermore, the ADC software, which was completely newly developed within the scope of this work, allows immediate insight into the acquired measurement data thanks to the graphic display, which has proven to be very helpful in the detailed analysis of the raw data: All information found during the data analysis (e.g. the T_i and the integration range as well as the size of the evaluated pulse) is directly displayed graphically, which considerably simplifies and accelerates the error diagnosis during signal acquisition (e.g. in the improvement of the signal evaluation in section 3.3.3, Figure 3.7, 3.8).

2.7.2 Archiving the ADC raw data

Modern computer systems with sufficient hard disk space easily allow the uncompressed raw signals to be stored. Especially during the development phase, the offline data is valuable for developing, testing and comparing improved analysis routines without requiring further measurement time at the accelerator. Also during routine operation, it has proven useful for fault diagnosis to save the status before and after each optimisation of the machine as raw data from the HF monitors.

The system also allows entire measurement sequences to be stored as raw data and later replayed in the same way as if the data actually came from the running accelerator. This makes it possible to analyse measurements once they have been carried out at later points in time, taking new findings into account. This way of dealing with the data from the beam diagnostic systems of an accelerator is thus similar to the procedure otherwise known from experiments in nuclear or high-energy physics. There, too, the measurement data of the experiment data acquisition are usually written to data storage in their raw version so that they can be evaluated at any time, taking new findings into account.

2.7.3 Data acquisition performance

If the data acquisition is fast enough, measurements can be made with comparatively greater detail. This shortens, for example, the acceptance measurements presented in section 4.3, in which a great many different machine configurations are examined, to about half the time.

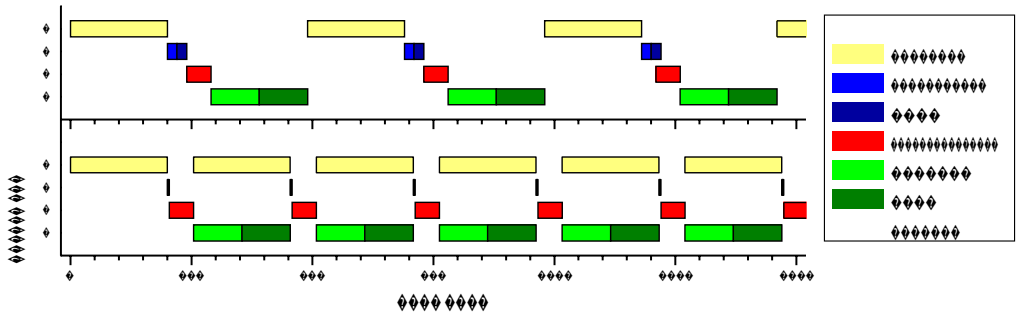

Figure 2.21:
Typical timing during HFMO data collection: First set the machine (1. yellow, ≈200 ms), then prepare ADC system (2. blue, ≈40 ms), digitise (3. red, ≈50 ms) and read out/analyse (4. green, ≈200 ms). The graphic below shows the optimised sequence: Only during the real data acquisition the machine is not changed.
It is clearly visible that with the optimised method in this example, about twice as many measurements can be carried out in the same period of time.

The previously always synchronously performed data acquisition takes place in four steps (Figure 2.21), which are performed each time for time-uncritical measurements. This means that such a measurement requires between 300 ms and 500 ms.

However, the process offers optimisation potential through parallelisation: If each measurement requires the same multiplexer and ADC channel configuration, the second step can be dispensed with. However, this can only save about 40 ms with completely synchronous data processing.

The state of the accelerator no longer plays a role for further processing after completion of the digitisation (step 3.) and can therefore already be used in parallel from step
4. ("dead time") can be changed. To do this, however, the measuring programme must be able to process the measurement data asynchronously. The procedure proves to be advantageous if the setting of a new accelerator configuration requires some 10 ms to 200 ms, so that the measurements can be carried out about two to four times faster.